Conformational Characteristics and Configurational Properties of Poly(ethylene imine-*alt*-ethylene sulfide) and the Role of the Secondary Amine Group as a Junction of Attractive Interactions

Yuji Sasanuma* and Ryota Kumagai

Department of Applied Chemistry and Biotechnology, Faculty of Engineering, Chiba University, 1-33 Yayoi-cho, Inage-ku, Chiba 263-8522, Japan

Received May 13, 2007; Revised Manuscript Received June 17, 2007

ABSTRACT: Conformational analysis of poly(ethylene imine-*alt*-ethylene sulfide) (PEIES) has been carried out from ab initio molecular orbital calculations and NMR experiments for its model compound, *N*-(2-methylthioethyl)methylamine (MTEMA). The *meso*-diad probability, bond conformations, and characteristic ratio of PEIES were predicted by the refined inversional−rotational isomeric state (IRIS) calculations using conformational energies determined from MTEMA. The refined IRIS scheme can treat geometrical parameters and interaction energies as a function of conformations of the present and neighboring bonds. The configurational properties of poly(ethylene imine-*alt*-ethylene oxide) (PEIEO), poly(*N*-methylethylene imine-*alt*-ethylene oxide), and poly(ethylene imine) (PEI) were also evaluated by the refined IRIS computations and compared with those obtained by the conventional method. So long as geometrical parameters are properly chosen, the conventional IRIS method may yield results comparable to those by the refined scheme. Spatial configurations of these polymers depend chiefly on intramolecular attractions between the heteroatoms; the characteristic ratio ($\langle r^2\rangle_0/nl^2$) inversely correlates with the strength of N−H···X (X = O, N, or S) attraction: PEIEO with N−H···O of −1.75 kcal mol^{-1}, $\langle r^2\rangle_0/nl^2$ = 1.33; PEI with N−H···N of −1.54 kcal mol^{-1}, 3.09; PEIES with N−H···S of −0.97 kcal mol^{-1}, 5.15.

1. Introduction

The secondary amine (NH) group, having a lone pair and a hydrogen atom, can play roles of both electron donor and acceptor and hence acts as a junction of intramolecular and intermolecular attractions to assemble higher-order structures, molecular aggregates, and supermolecules. Amine groups, depending on pH, tend to be protonated, thus exerting electrostatic forces as well as the above-mentioned attractions and van der Waals forces.[1]

Poly(ethylene imine) (PEI) forms an attractive interaction between the NH sites (N−H···N, −1.54 kcal mol^{-1}),[2] and poly(ethylene imine-*alt*-ethylene oxide) (PEIEO) shows a stronger attraction (N−H···O, −1.75 kcal mol^{-1}).[3] These intramolecular attractions substantially determine their conformational characteristics, configurational properties, higher-order structures, and physical properties. Sulfur may be the third object to be investigated as a partner of the NH group, because sulfur has lone pairs and is frequently found in synthetic and biological polymers.

This study has dealt with poly(ethylene imine-*alt*-ethylene sulfide) (PEIES, see Figure 1). Ab initio molecular orbital (MO) calculations and proton and carbon-13 NMR experiments for its model compound, *N*-(2-methylthioethyl)methylamine (MTEMA), were carried out to evaluate the conformer free energies and bond conformations, and the theoretical and experimental data were compared. For nitrogenous polymers, we have developed the inversional−rotational isomeric state (IRIS) scheme and applied it to PEI,[2] poly(trimethylene imine),[4] poly(*N*-methyltrimethylene imine),[4] PEIEO,[3] and poly(*N*-methylethylene imine-*alt*-ethylene oxide) (PMEIEO).[3] In addition, we have recently proposed the refined rotational isomeric state (RIS) scheme that includes the dependence of geometrical parameters as well as interaction energies on conformations of the current and neighboring bonds.[5] The refined RIS calculations exactly reproduced configurational properties of poly(ethylene oxide-*alt*-ethylene sulfide) (PEOES) from purely theoretical conformational energies and geometrical parameters of its model compound. In a series of studies, we have demonstrated that polymers can be fully characterized by means of their model compounds.

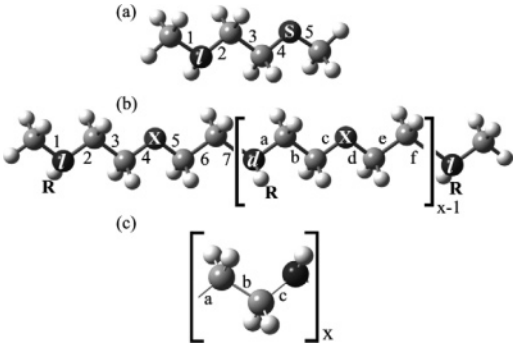

Figure 1. All-trans states of (a) *N*-(2-methylthioethyl)methylamine (MTEMA), (b) poly(ethylene imine-*alt*-ethylene sulfide) (PEIES, R = H, X = S), poly(ethylene imine-*alt*-ethylene oxide) (PEIEO, R = H, X = O), or poly(*N*-methylethylene imine-*alt*-ethylene oxide) (PMEIEO, R = CH_3, X = O), and (c) poly(ethylene imine) (PEI). The bonds are labeled as indicated. The *l* and *d* forms are defined as follows. The polymer in the all-trans state is put on paper as shown. When the hydrogen atom of the most left-hand NR group appears on this (that) side of the paper, the nitrogen site is considered to adopt the *d* (*l*) form. For other nitrogen sites, the *d* and *l* configurations are defined similarly. The *dd* and *ll* forms are referred to as *meso*, and *dl* and *ld* as *racemo*.

In this study, the IRIS scheme has been combined with the refined RIS treatment. This improved methodology is hereafter referred to as the *refined* IRIS scheme to discriminate it from the *conventional* method. The refined IRIS scheme, treating the

* To whom correspondence should be addressed. E-mail: sasanuma@faculty.chiba-u.jp

10.1021/ma071077b CCC: $37.00
Published on Web 08/17/2007

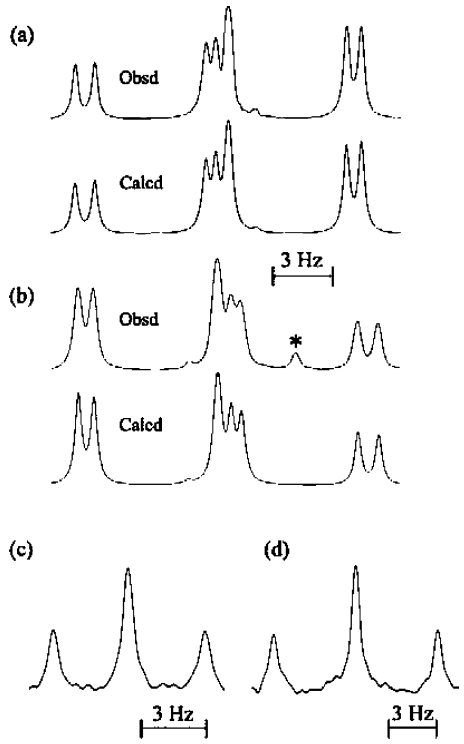

Figure 2. ^{1}H NMR spectra of methylene protons, (a) AA′ and (b) BB′, and ^{13}C NMR spectra of methyl carbons, (c) CH_3N- and (d) CH_3S-, of MTEMA dissolved in CD_3OD at 25 °C. The asterisk expresses a peak from impurities. For designations of the hydrogen atoms, see Figure 3b.

nitrogen inversion as well as geometrical parameters and interactions as a function of conformations of the current and neighboring bonds, enables us to rigorously characterize polymers containing NR groups (R: substituent) in the main chain. Here, the refined IRIS scheme has been applied to not only PEIES but also PEIEO, PMEIEO, and PEI to investigate their conformational characteristics, configurational properties, and secondary structures and furthermore to correlate these characteristic features with intramolecular interactions due to the heteroatoms. The results are compared with those obtained by the conventional IRIS method, and the validity of the conventional method is discussed.

2. Computations and Experiments

2.1. Ab Initio MO Calculations. Ab initio MO calculations were carried out with the Gaussian03 program[6] installed on an HPC Silent-SCC T2 or an HPC SCC System-L computer. For each conformer of MTEMA, the geometrical parameters were fully optimized at the HF/6-31G(d) level, and the thermal correction to the Gibbs free energy (at 25 °C and 1 atm) was calculated with a calibration factor of 0.9135.[7] With the optimized geometry, the self-consistent field (SCF) energy was computed at the MP2/6-311++G(3df, 3pd) level. All the SCF calculations were performed under the tight convergence. The Gibbs free energy was evaluated from the SCF and thermal-correction energies, being given here as the difference from that of the all-trans conformer and denoted as ΔG_k (k: conformer). In addition, NMR coupling constants of MTEMA were calculated at the B3LYP/6-311++G(3df, 3pd)//B3LYP/6-31G(d) level.

Bond lengths, bond angles, and dihedral angles used in the refined IRIS computations for PEIES, PEIEO, PMEIEO, and PEI were determined by geometrical optimizations at the B3LYP/6-31G(d) level for conformers of $CH_3CH_2NHCH_2CH_2SCH_2CH_3$, $CH_3CH_2NHCH_2CH_2OCH_2CH_3$, $CH_3CH_2N(CH_3)CH_2CH_2OCH_2CH_3$, and *ll*-$CH_3CH_2NHCH_2CH_2NHCH_2CH_3$ and *ld*-$CH_3CH_2NHCH_2CH_2NHCH_2CH_3$, respectively.[8]

Table 1. Observed Vicinal ^{1}H−^{1}H and ^{13}C−^{1}H Coupling Constants of MTEMA[a]

solvent	$^3J_{HH}$	$^3J'_{HH}$	$^3J_{CH}^{CN}$	$^3J_{CH}^{CS}$
C_6D_{12}	6.71	6.00	3.68	4.88
$CDCl_3$	6.67	6.26	3.75	4.64
CD_3OD	7.20	6.47	3.71	4.73
$(CD_3)_2SO$	7.85	6.14	4.13	4.62

[a] In Hz. At 25 °C.

2.2. Sample Preparation. *N*-(2-Methylthioethyl)methylamine was prepared as follows. α-Methylthioacetic acid was chlorinated with thionyl chloride to give α-methylthioacetyl chloride,[9] the product was reacted with methylamine to form *N*-methyl-α-(methylthio)acetamide,[10] and the acetamide was reduced with lithium aluminum hydride to yield MTEMA.[11] 3-Methyl-1,4-thiazane (MTZ) was prepared according to Gallego et al.[12]

2.3. NMR Measurements. ^{1}H (^{13}C) NMR spectra were measured at 500 MHz (126 MHz) on a JEOL JNM-LA500 spectrometer equipped with a variable temperature controller in the Chemical Analysis Center of Chiba University. The experimental conditions were the same as those in previous studies.[2−5] The solvents were cyclohexane-d_{12} (C_6D_{12}), chloroform-d ($CDCl_3$), methanol-d_4 (CD_3OD), and dimethyl-d_6 sulfoxide ($(CD_3)_2SO$), and the solute concentration was ca. 5 vol %. The NMR spectra were simulated with the gNMR program[13] to derive the chemical shifts and coupling constants.

3. Results and Discussion

3.1. ^{1}H NMR. Figure 2 shows ^{1}H NMR spectra observed from methylene protons of MTEMA. The gNMR simulations gave two vicinal coupling constants, $^3J_{HH}$ ($=^3J_{AB} = {}^3J_{A'B'}$) and $^3J'_{HH}$ ($=^3J_{AB'} = {}^3J_{A'B}$), as listed in Tables 1 and S1 (Supporting Information). The observed coupling constants are expressed as

$$^3J_{HH} = {}^3J_G^{HH}\, p_t^{CC} + \frac{{}^3J_T'^{HH} + {}^3J_G''^{HH}}{2} p_g^{CC} \quad (1)$$

and

$$^3J'_{HH} = {}^3J_T^{HH}\, p_t^{CC} + \frac{{}^3J_G'^{HH} + {}^3J_G'''^{HH}}{2} p_g^{CC} \quad (2)$$

where $^3J_T^{HH}$'s and $^3J_G^{HH}$'s are defined in Figure 3, and p_t^{CC} and p_g^{CC} are trans and gauche fractions of the C−C bond, respectively. Therefore, we have

$$p_t^{CC} + p_g^{CC} = 1 \quad (3)$$

As $^3J^{HH}$'s in eqs 1 and 2, we have used those obtained from the $N-CH_2-CH_2-S$ bond sequence of MTZ. In Figure 4, as an example, its observed and calculated ^{1}H NMR spectra are compared. Listed in Table 2 are the vicinal coupling constants derived from the gNMR simulations. The p_t^{CC} and p_g^{CC} values were obtained from eqs 1 and 2 and divided by their sum to satisfy eq 3. The experimental p_t^{CC} values are shown in Table 3; for the temperature dependence, see Table S2 (Supporting Information).

3.2. ^{13}C NMR. Figure 2 also shows observed ^{13}C NMR spectra of methyl carbons of MTEMA. The triplets are due to the vicinal couplings of $^{13}CH_3-N-CH_2$ ($^3J_{CH}^{CN}$) or $^{13}CH_3-S-CH_2$ ($^3J_{CH}^{CS}$). The $^3J_{CH}^{CX}$ (X = N or S) values for the four solutions are listed in Tables 1 and S1. The observed value can be expressed as

$$^3J_{CH}^{CX} = {}^3J_G^{CH}\, p_t^{CX} + \frac{{}^3J_T'^{CH} + {}^3J_G'^{CH}}{2} p_g^{CX} \quad (4)$$

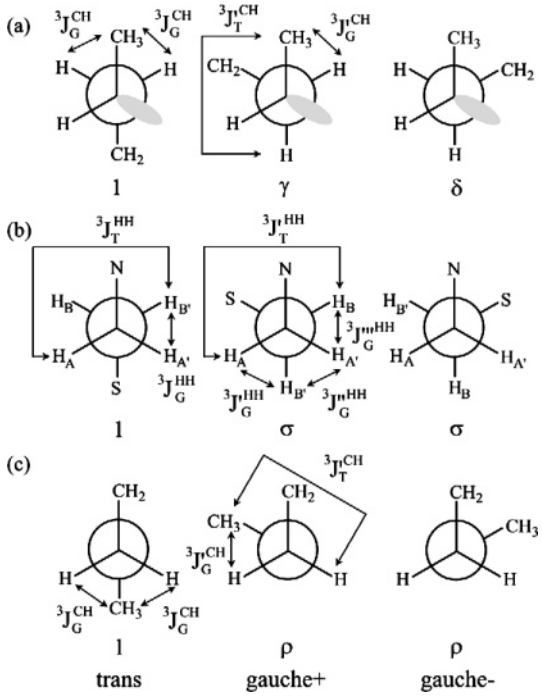

Figure 3. Rotational isomeric states around the (a) NH−CH_2, (b) CH_2−CH_2, and (c) CH_2−S bonds of MTEMA with definitions of vicinal coupling constants. The Greek letters represent first-order interactions.

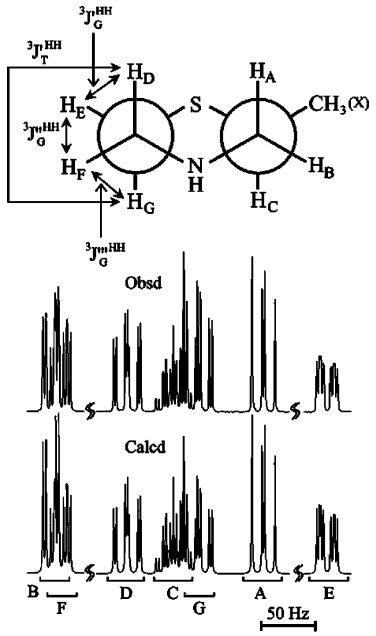

Figure 4. ^{1}H NMR spectra of 3-methyl-1,4-thiazane (MTZ) dissolved in C_6D_{12} at 25 °C. The peaks were assigned as shown. The NMR parameters were determined as follows (δ relative to $\delta_{C_6D_{12}}$ in ppm and J in Hz): $\delta_A = 2.57$, $\delta_B = 3.12$, $\delta_C = 2.73$, $\delta_D = 2.82$, $\delta_E = 2.32$, $\delta_F = 3.10$, $\delta_G = 2.69$, $\delta_X = 1.08$, $^2J_{AB} = -12.07$, $^3J_{AC} = 9.58$, $^3J_{BC} = 2.91$, $^3J_{DE} = 2.49$, $^2J_{DF} = -12.08$, $^3J_{DG} = 10.83$, $^3J_{EF} = 3.77$, $^2J_{EG} = -13.06$, $^3J_{FG} = 3.01$, and $^3J_{CX} = 6.90$.

where $^3J'_T{}^{CH}$ and $^3J_G^{CH}$'s are defined in Figure 3, and p_t^{CX} and p_g^{CX} are trans and gauche fractions of the C−X bond, respectively. For X = N, to derive the p_t^{CN} values, the $^3J_G^{CH}$, $^3J'_T{}^{CH}$, and $^3J'_G{}^{CH}$ values obtained from model compounds of PEI and poly(*N*-methylethylene imine)[2] have been used. For X = S, the $^3J_T^{CH}$ and $^3J_G^{CH}$ values of 2-methyl-1,3,5-trithiane[14] were tentatively used on the assumption that $^3J_G^{CH} = {}^3J'_G{}^{CH}$. For example, substitution of $^3J'_T{}^{CH} = 7.13$, $^3J_G^{CH} = {}^3J'_G{}^{CH} = 2.62$, and $^3J_{CH}^{CX} =$ 4.91 Hz (C_6D_{12} at 15 °C) into eq 4 yielded a negative p_t^{CS} value of −0.02. Similar results were obtained from 2-methoxyethyl methyl sulfide,[5] a model compound of PEOES. The MO calculations on NMR parameters of MTEMA gave a large difference between $^3J_G^{CH}$ (1.84 Hz) and $^3J'_G{}^{CH}$ (3.83 Hz); therefore, the negative p_t^{CS} value stems from the assumption of $^3J_G^{CH} = {}^3J'_G{}^{CH}$. For X = S, therefore, the above $^3J_G^{CH}$ and $^3J'_G{}^{CH}$ values and $^3J'_T{}^{CH} = 7.35$ Hz, obtained from the MO calculations, have been adopted. The p_t^{CN} and p_t^{CS} values thus derived are also listed in Tables 3 and S2 (Supporting Information).

Table 2. Vicinal ^{1}H−^{1}H Coupling Constants of MTZ[a]

solvent	$^3J'_T{}^{HH}$	$^3J'_G{}^{HH}$	$^3J''_G{}^{HH}$	$^3J'''_G{}^{HH}$	$^3J_G^{HH}$
C_6D_{12}	10.83	2.49	3.77	3.01	3.09
$CDCl_3$	11.38	2.45	3.55	2.97	2.99
CD_3OD	11.50	3.01	3.26	2.64	2.97
$(CD_3)_2SO$	10.90	1.90	3.75	3.30	2.98

[a] In Hz. At 25 °C. For definitions of the coupling constants, see Figure 4. $^3J_T^{HH} = {}^3J'_T{}^{HH}$ and $^3J_G^{HH} = (^3J'_G{}^{HH} + {}^3J''_G{}^{HH} + {}^3J'''_G{}^{HH})/3$.

Table 3. Bond Conformations of MTEMA and PEIES[a]

	medium	permittivity	HBS (%)	p_t^{CN}	p_t^{CC}	p_t^{CO}
		MO Calculated				
MTEMA	gas phase	1.0		0.70	0.26	0.25
		NMR Experimental				
	C_6D_{12}	2.0		0.89	0.32	0.19
	$CDCl_3$	4.8		0.84	0.33	0.25
	CD_3OD	32.7		0.79	0.30	0.23
	$(CD_3)_2SO$	46.7		0.67	0.27	0.26
		IRIS				
PEIES			100	0.73	0.27	0.35
			80	0.72	0.33	0.34
			60	0.70	0.39	0.33
			40	0.69	0.45	0.32
			20	0.67	0.51	0.31
			0	0.66	0.56	0.30

[a] At 25 °C.

3.3. Conformational Energies of MTEMA. Statistical weight matrices, U_j (j: bond number), of MTEMA are given in Appendix A (Supporting Information). The conformer free energies of the *l* form, obtained from the MO calculations, are tabulated in Table 4, together with the statistical weights. Here, the *l* and *d* forms are defined according to the pseudoasymmetry (see Figure 1).[15,16] The first-, second-, and third-order interactions of MTEMA (PEIES) are illustrated in Figures 3 and 5. The statistical weight is related to the corresponding conformational energy by, for example, $\sigma = \exp(-E_\sigma/RT)$, where R is the gas constant, and T is the absolute temperature.[17,18] The conformational energies, determined by the least-squares method for the ΔG_k values as described previously,[4] are compared with those of PEIEO, PMEIEO, PEI, PES, and their model compounds (Table 5).

The first-order interaction energies (E_γ and E_δ) around the C−N bond of MTEMA are close to those of *N*-(2-methoxyethyl)methylamine (MEMA) and *N*,*N*′-dimethylethylenediamine (di-MEDA), and MTEMA has the same E_ρ value as 1,2-bis(methylthio)ethane (BMTE). Bonds of the same kind seem to have similar first-order interaction energies, except for the C−C bond of BMTE. Its large E_σ value is due to the S···S repulsion occurring in the C−C gauche conformation.[19] In contrast, there are a variety of second- and third-order interaction energies. In Table 5, only attractive interactions are boldfaced. The strength of the N−H···X (η) attraction (see Figure 5) is evaluated to be on the order of $E_\eta = -0.97$ (X = S) → −1.54 (X = N) → −1.75 (X = O) kcal mol^{-1}. In MTEMA, the long C−S bonds

Table 4. Conformer Free Energies of *l*-MTEMA, Evaluated from Ab Initio MO Calculations

k	conformation	statistical weight[a]	ΔG_k[b] (kcal mol^{-1})
1	t t t	1	0.00
2	t t g$^+$	ρ	−0.22
3	t t g$^-$	ρ	−0.41
4	t g$^+$ t	$\sigma\nu'$	0.58
5	t g$^+$ g$^+$	$\rho\sigma\nu'$	0.88
6	t g$^+$ g$^-$	$\rho\sigma\nu'\omega'$	0.38
7	t g$^-$ t	$\sigma\eta$	−0.78
8	t g$^-$ g$^+$	$\rho\sigma\eta\omega'_H$	−0.38
9	t g$^-$ g$^-$	$\rho\sigma\eta$	−1.40
10	g$^+$ t t	γ	0.76
11	g$^+$ t g$^+$	$\gamma\rho$	0.48
12	g$^+$ t g$^-$	$\gamma\rho$	0.44
13	g$^+$ g$^+$ t	$\gamma\sigma\eta$	−0.18
14	g$^+$ g$^+$ g$^+$	$\gamma\rho\sigma\eta$	−0.65
15	g$^+$ g$^+$ g$^-$	$\gamma\rho\sigma\eta\omega'_H$	0.69
16	g$^+$ g$^-$ t	$\gamma\sigma\omega$	1.71
17	g$^+$ g$^-$ g$^+$	$\gamma\rho\sigma\omega\omega'_H$	3.30
18	g$^+$ g$^-$ g$^-$	$\gamma\rho\sigma\omega$	2.20
19	g$^-$ t t	δ	0.34
20	g$^-$ t g$^+$	$\delta\rho$	−0.04
21	g$^-$ t g$^-$	$\delta\rho$	0.13
22	g$^-$ g$^+$ t	$\delta\sigma\omega$	1.35
23	g$^-$ g$^+$ g$^+$	$\delta\rho\sigma\omega$	1.37
24	g$^-$ g$^+$ g$^-$	0[c]	
25	g$^-$ g$^-$ t	$\delta\sigma\nu'$	0.71
26	g$^-$ g$^-$ g$^+$	$\delta\rho\sigma\nu'\omega'$	0.55
27	g$^-$ g$^-$ g$^-$	$\delta\rho\sigma\nu'$	1.21

[a] For the intramolecular interactions, see Figures 3 and 5. [b] At the MP2/6-311++G(3df, 3pd)//HF/6-31G(d) level. Relative to the G_k value of the all-trans conformation. [c] The geometrical optimization did not detect the potential minimum; thus, the g$^-$ g$^+$ g$^-$ conformer is considered to be absent.

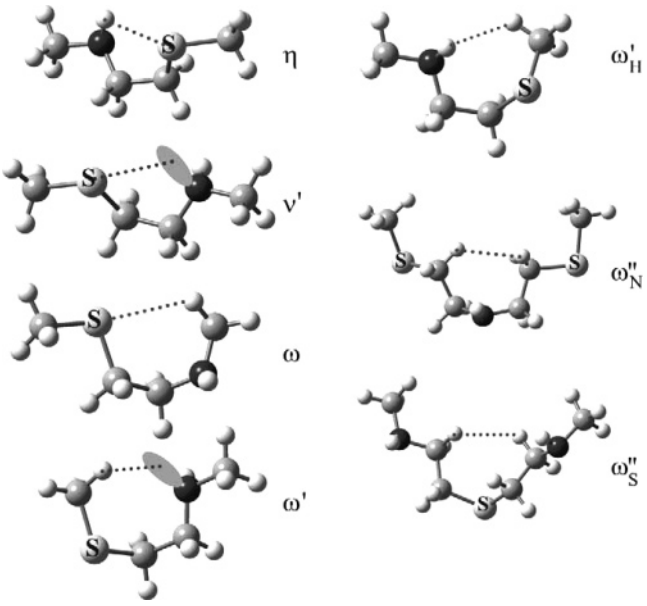

Figure 5. Second- and third-order intramolecular interactions defined for MTEMA and PEIES.

render the (C−H)···O interaction of no effect: $E_{\omega'} \approx 0$. Bond conformations (trans fractions) of MTEMA, calculated from the ΔG_k values as in previous studies,[20] are listed in Tables 3 and S2. Its C−N, C−C, and C−S bonds have the trans, gauche, and gauche preferences, respectively. The satisfactory agreement between the calculated and observed p_t values permits us to carry out conformational analysis of PEIEO using the MO calculations.[21]

3.4. Refined IRIS Scheme. The diad probabilities and bond conformations, being independent of the geometrical parameters, can be evaluated as described in section 3.9 of ref 2 and section 3.5 of ref 4. For PEIES, PEIEO, and PMEIEO, the statistical weight matrices are chosen for the individual diads (*ll*, *dd*, *ld*, and *dl*) according to Table 6 of ref 3. The characteristic ratio, $\langle r^2\rangle_0/nl^2$, can be calculated in the following manner.

Table 5. Conformational Energies (kcal mol^{-1}) of MTEMA (PEIES), MEMA (PEIEO), MEDA (PMEIEO), di-MEDA (PEI), and BMTE (PES), Derived from Ab Initio MO Calculations[a]

	MTEMA (PEIES)	MEMA (PEIEO)	MEDA (PMEIEO)	di-MEDA (PEI)	BMTE (PES)
		First-Order Interaction			
E_γ	0.77	1.06	1.52	1.06	
E_δ	0.37	0.44		0.54	
E_σ	0.01	0.05	0.03	−0.09	0.89
E_ρ	C−S: −0.40	C−O: 1.21	C−O: 1.27		C−S: −0.41
		Second- and Third-Order Interactions			
E_η	**−0.97**	**−1.75**		**−1.54**	
E_ν				**−0.58**	
$E_{\nu'}$	0.73	0.59	0.30	1.16	
E_ω	1.19	**−0.21**	**−0.41**	0.97	
$E_{\omega'}$	−0.05	**−0.68**	**−0.66**	0.61	
$E_{\omega'H}$	1.02				
$E_{\omega''N}$[b]	0.59	1.24	0.41	0.94	
$E_{\omega''S}$[b]	0.82				

[a] Abbreviations: MTEMA, *N*-(2-methylthioethyl)methylamine; PEIES, poly(ethylene imine-*alt*-ethylene sulfide); MEMA, *N*-(2-methoxyethyl)methylamine; PEIEO, poly(ethylene imine-*alt*-ethylene oxide); MEDA, *N*,*N*-(2-methoxyethyl)dimethylamine; PMEIEO, poly(*N*-methylethylene imine-*alt*-ethylene oxide); di-MEDA, *N*,*N*′-dimethylethylenediamine; PEI, poly(ethylene imine); BMTE, 1,2-bis(methylthio)ethane; PES, poly(ethylene sulfide). For definitions of the interactions, see Figures 3 and 5. The boldfaced figures represent the attractive interactions. [b] Evaluated from dimeric model compounds (see Figure 5).

Table 6. Characteristic Ratios Obtained from Refined and Conventional IRIS Calculations[a]

					conventional IRIS	
		HBS[b], %	P_m[c]	refined IRIS	case I[d]	case II[e]
PEIES	$\langle r^2\rangle_0/nl^2$	100	0.49	5.15	4.82	
		80	0.49	5.62	5.28	
		60	0.49	5.99	5.65	
		40	0.50	6.24	5.90	
		20	0.50	6.37	6.02	
		0	0.50	6.40	6.05	
	10^3d(ln $\langle r^2\rangle_0$)/dT, K^{-1}	100		0.96	0.65	
PEIEO	$\langle r^2\rangle_0/nl^2$	100	0.50	1.33	1.28	1.49
		80	0.50	1.96	1.92	2.18
		60	0.50	2.93	2.91	3.19
		40	0.50	4.25	4.23	4.45
		20	0.50	5.72	5.66	5.65
		0	0.50	6.94	6.75	6.47
	10^3d(ln $\langle r^2\rangle_0$)/dT, K^{-1}	100		8.6	8.2	8.2
PMEIEO	$\langle r^2\rangle_0/nl^2$	100	0.50	5.64	5.61	5.23
		80	0.50	5.74	5.71	5.37
		60	0.50	5.83	5.78	5.51
		40	0.50	5.91	5.86	5.65
		20	0.50	5.99	5.93	5.85
		0	0.50	6.06	6.00	5.92
	10^3d(ln $\langle r^2\rangle_0$)/dT, K^{-1}	100		−0.79	−0.62	−0.47
PEI	$\langle r^2\rangle_0/nl^2$	100	0.63	3.09	2.90	2.87
		80	0.61	3.50	3.31	3.25
		60	0.59	4.11	3.90	3.81
		40	0.56	4.95	4.71	4.54
		20	0.54	6.06	5.64	5.40
		0	0.52	7.32	6.63	6.29
	10^3d(ln $\langle r^2\rangle_0$)/dT, K^{-1}	100		2.7	2.5	2.2

[a] At 25 °C. [b] HBS: hydrogen bond strength. The attractive interaction energies E_ξ's ($\xi = \eta$ for PEIES, η, ω, and ω' for PEIEO, ω and ω' for PMEIEO, and η and ν for PEI, see Table 5) were multiplied by a factor of HBS/100 to be used in the calculations. [c] *meso*-Diad probability. [d] Using the averaged geometrical parameters listed in Tables S3 and S4 (Supporting Information). [e] Using the geometrical parameters adopted from typical conformers of model compounds: PEIEO and PMEIEO, Table 7 of ref 3; PEI, Table 8 of ref 2.

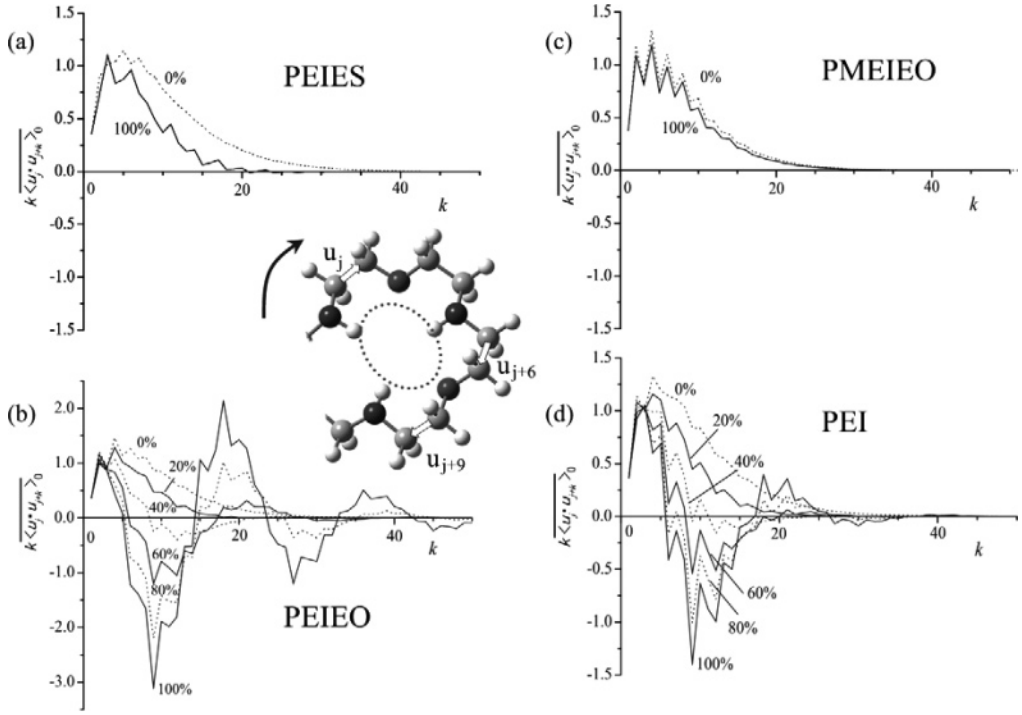

Figure 6. $k\overline{\langle \mathbf{u}_j \cdot \mathbf{u}_{j+k}\rangle_0}$ vs k curves of (a) PEIES, (b) PEIEO, (c) PMEIEO, and (d) PEI. The percentage represents the hydrogen bond strength (HBS).

The H_i matrices (defined in eqs 17 and 18 of ref 5) are prepared for the individual diads. The configurational sequence of the polymeric chain is so determined by the Monte Carlo method as to match the calculated *meso*-diad probability.[2,4] From the H_i matrices arranged according to the diad sequence generated, the characteristic ratio $\langle r^2\rangle_0/nl^2$ is calculated as described in section 3.2 of ref 5. The above process is performed for all chains in the system (the number of chains is n_c). The $\langle r^2\rangle_0/nl^2$ values of the n_c chains are averaged to yield the mean chain dimension of the ensemble.[22] These computations were performed for PEIES, PEIEO, PMEIEO, and PEI.

To correlate the chain dimension with the attractive forces, the conformational energies boldfaced in Table 5 were multiplied by a factor of HBS (%)/100 (HBS: hydrogen bond strength)[23] and used in the calculations; HBS = 100% corresponds to the energies as in Table 5, and HBS = 0% to null energies. The temperature was set equal to 25 °C. The *meso*-diad probabilities, P_m's, are listed in Table 6. Inasmuch as nitrogen sites of PEIES, PEIEO, and PMEIEO are separated by six bonds, these polymeric chains are essentially atactic ($P_m = 0.50$). On the other hand, PEI prefers the *meso* configuration at high HBSs. As HBS decreases, however, PEI becomes atactic. The characteristic ratios calculated as above are given in the column of "refined IRIS" of Table 6. The $\langle r^2\rangle_0/nl^2$ values were derived from the extrapolation of $x^{-1} \rightarrow 0$ of $\langle r^2\rangle_0/nl^2$ vs x^{-1} plots, representing the infinite chains ($x \rightarrow \infty$). The PEIEO, PEI, and PEIES chains give $\langle r^2\rangle_0/nl^2$ values of 1.33, 3.09, and 5.15 at HBS = 100%, respectively. The chain dimension seems to be inversely correlated to the strength of the N−H···X (η) attraction. The PMEIEO chain, of which nitrogen site is blocked with a methyl group and does not form the η interaction, is as extended as $\langle r^2\rangle_0/nl^2 = 5.64$. At HBS = 0% all the chains show close dimensions of $\langle r^2\rangle_0/nl^2 = 6-7$.[24]

While the refined IRIS computations were performed, the bond lengths, bond angles, and dihedral angles were averaged with the conformational probabilities calculated from the statistical weight matrices used as the weights;[22] therefore, the average values depend on temperature and conformational energies. By way of example, the geometrical parameters at 25 °C and HBS = 100% are shown in Tables S3 and S4 (Supporting Information). The characteristic ratios were recomputed by the conventional IRIS method using the geometrical parameters averaged for the individual HBSs, being listed in the column of "case I" of Table 6. The differences in $\langle r^2\rangle_0/nl^2$ between refined IRIS and case I are allowably small. The results of the previous studies are also shown in the column of "case II" of Table 6; then, the bond lengths and bond angles were adopted from the all-trans conformations of the model compounds, and the dihedral angles from their typical conformers such as ttt, $g^{\pm}$tt, $tg^{\pm}$t, and $ttg^{\pm}$. For case II, the deviations from refined IRIS are not necessarily permissible, and the characteristic ratio of PEIEO is somewhat overestimated whereas those of PMEIEO and PEI are rather underestimated. In contrast, the refined RIS scheme consistently yields larger temperature coefficients than the conventional method. On balance, however, this study has justified the conventional IRIS (RIS) scheme, although we must consider how to determine the geometrical parameters and pay attention to tolerances of the obtained data.

3.5. Orientation Correlation between Bonds and Secondary Structure. The scalar product between unit vectors $\mathbf{u}_j$ and $\mathbf{u}_{j+k}$ along bonds j and $j + k$ can be used as a measure of the orientation correlation between the two bonds[3,25]

$$k\overline{\langle \mathbf{u}_j \cdot \mathbf{u}_{j+k}\rangle_0} = k\overline{\langle \cos\theta_{j,j+k}\rangle_0} \tag{5}$$

where $\theta_{j,j+k}$ is the angle between the two vectors (bonds). The amplification factor k is introduced to enhance the long-range correlations. The overbar stands for the average for the skeletal bonds and configurations, the angular brackets represent the average over all possible conformations, and the subscript 0 indicates the unperturbed state. The $k\overline{\langle \mathbf{u}_j \cdot \mathbf{u}_{j+k}\rangle_0}$ terms of PEIES, PEIEO, PMEIEO, and PEI, calculated with the averaged geometrical parameters of case I (Tables S3 and S4, Supporting Information), are plotted against k in Figure 6. The $k\overline{\langle \mathbf{u}_j \cdot \mathbf{u}_{j+k}\rangle_0}$ vs k curves are analogous in profile to those obtained previously[3]

from the geometrical parameters of case II but somewhat different in numerical value. The $k\langle \mathbf{u}_j \cdot \mathbf{u}_{j+k} \rangle_0$ curves of PEIEO and PEI of HBS = 100% show such long-period undulations as to intersect the horizontal line around $k = 5-6$ and take the minimum at $k = 9$ and the maximum at $k = 18$; therefore, the $\mathbf{u}_j$ vector may be perpendicular to $\mathbf{u}_{j+5}$ or $\mathbf{u}_{j+6}$, antiparallel to $\mathbf{u}_{j+9}$, and parallel to $\mathbf{u}_{j+18}$. These results show that the PEIEO chain in particular tends to include fragments of a circular (or helical) structure of ca. 18 bonds per turn, as illustrated in Figure 6. Inasmuch as the undulation fades away with decreasing HBS, the circular structure stems from the N−H···O attractions. The PEI chain behaves similarly. In contrast, the curves of PEIES and PMEIEO monotonously decrease with increasing k even at HBS = 100%; the attractive interactions of PEIES and PMEIES are not so effective as to keep such a secondary structure.

Acknowledgment. This work was partly supported by the Asahi Glass Foundation and a Grant-in-Aid for Scientific Research (B) (18350112) from the Japan Society for the Promotion of Science.

Supporting Information Available: Vicinal coupling constants and bond conformations of MTEMA as a function of temperature (Tables S1 and S2), averaged geometrical parameters of PEIES, PEIEO, PMEIEO, and PEI (Tables S3 and S4) and statistical weight matrices of MTEMA and PEIES (Appendix A). This material is available free of charge via the Internet at http://pubs.acs.org.

References and Notes

(1) Here, the polymers and model compounds are assumed to be dissolved in organic solvents and hence not to be protonated.
(2) Sasanuma, Y.; Hattori, S.; Imazu, S.; Ikeda, S.; Kaizuka, T.; Iijima, T.; Sawanobori, M.; Azam, M. A.; Law, R. V.; Steinke, J. H. G. *Macromolecules* **2004**, *37*, 9169.
(3) Sasanuma, Y.; Kumagai, R.; Nakata, K. *Macromolecules* **2006**, *39*, 6752.
(4) Sasanuma, Y.; Teramae, F.; Yamashita, H.; Hamano, I.; Hattori, S. *Macromolecules* **2005**, *38*, 3519.
(5) Sasanuma, Y.; Asai, S.; Kumagai, R. *Macromolecules* **2007**, *40*, 3488.
(6) Frisch, M. J.; Trucks, G. W.; Schlegel, H. B.; Scuseria, G. E.; Robb, M. A.; Cheeseman, J. R.; Montgomery, J. A., Jr.; Vreven, T.; Kudin, K. N.; Burant, J. C.; Millam, J. M.; Iyengar, S. S.; Tomasi, J.; Barone, V.; Mennucci, B.; Cossi, M.; Scalmani, G.; Rega, N.; Petersson, G. A.; Nakatsuji, H.; Hada, M.; Ehara, M.; Toyota, K.; Fukuda, R.; Hasegawa, J.; Ishida, M.; Nakajima, T.; Honda, Y.; Kitao, O.; Nakai, H.; Klene, M.; Li, X.; Knox, J. E.; Hratchian, H. P.; Cross, J. B.; Bakken, V.; Adamo, C.; Jaramillo, J.; Gomperts, R.; Stratmann, R. E.; Yazyev, O.; Austin, A. J.; Cammi, R.; Pomelli, C.; Ochterski, J. W.; Ayala, P. Y.; Morokuma, K.; Voth, G. A.; Salvador, P.; Dannenberg, J. J.; Zakrzewski, V. G.; Dapprich, S.; Daniels, A. D.; Strain, M. C.; Farkas, O.; Malick, D. K.; Rabuck, A. D.; Raghavachari, K.; Foresman, J. B.; Ortiz, J. V.; Cui, Q.; Baboul, A. G.; Clifford, S.; Cioslowski, J.; Stefanov, B. B.; Liu, G.; Liashenko, A.; Piskorz, P.; Komaromi, I.; Martin, R. L.; Fox, D. J.; Keith, T.; Al-Laham, M. A.; Peng, C. Y.; Nanayakkara, A.; Challacombe, M.; Gill, P. M. W.; Johnson, B.; Chen, W.; Wong, M. W.; Gonzalez, C.; Pople, J. A. *Gaussian03*, revision D.01; Gaussian, Inc.: Wallingford CT, 2004.
(7) Pople, J. A.; Scott, A. P.; Wong, M. W.; Radom, L. *Isr. J. Chem.* **1993**, *33*, 345.
(8) For each mode compound, 63 conformers were optimized. A large number of data were obtained, thus not being shown here.
(9) Ryu, Z. H.; Shin, S. H.; Lee, J. P.; Lim, G. T.; Bentley, T. W. *J. Chem. Soc., Perkin Trans. 2* **2002**, 1283.
(10) Tamura, Y.; Maeda, H.; Choi, H. D.; Ishibashi, H. *Synthesis* **1982**, 56.
(11) Mndzhoyan, A. L.; Afrikyan, V. G.; Badalyan, V. E.; Markaryan, E. A.; Khorenyan, G. A. *Dokl. Akad. Nauk Armyan. SSR* **1958**, *27*, 161.
(12) Gallego, M. T.; Brunet, E.; Ruano, J. L. G.; Eliel, E. L. *J. Org. Chem.* **1993**, *58*, 3905.
(13) Budzelaar, P. H. M. *gNMR*, version 5.0. IvorySoft & Adept Scientific plc: Letchworth, U.K., 2004.
(14) Sawanobori, M.; Sasanuma, Y.; Kaito, A. *Macromolecules* **2001**, *34*, 8321.
(15) Flory, P. J.; Mark, J. E.; Abe, A. *J. Am. Chem. Soc.* **1966**, *88*, 639.
(16) Flory, P. J. *J. Am. Chem. Soc.* **1967**, *89*, 1798.
(17) Flory, P. J. *Statistical Mechanics of Chain Molecules*; Wiley & Sons: New York, 1969.
(18) Mattice, W. L.; Suter, U. W. *Conformational Theory of Large Molecules: The Rotational Isomeric State Model in Macromolecular Systems*; Wiley & Sons: New York, 1994.
(19) Sasanuma, Y.; Ohta, H.; Touma, I.; Matoba, H.; Hayashi, Y.; Kaito, A. *Macromolecules* **2002**, *35*, 3748.
(20) See, for example: Sasanuma, Y. *Macromolecules* **1995**, *28*, 8629.
(21) The MO calculations agree well with the NMR observations using the polar solvent, $(CD_3)_2SO$. The N−H···X (X = S, O, or N) attraction affects the p_t^{CC} value in particular (see, for example, the p_t^{CC} values for different HBSs of PEIES in Table 3). The N−H···S attraction may differ from the N−H···N and N−H···O ones in solvent dependence. The N−H···N interaction becomes weak (the p_t^{CC} value increases) with increasing solvent polarity, whereas the N−H···O attraction is too strong to be influenced by solvent.
(22) The probability $p_{\alpha\beta\gamma,j,n_2}$ that the n_2th polymeric chain adopts α, β, and γ conformations at bonds $j-1$, j, and $j+1$, respectively, is given by

$$p_{\alpha\beta\gamma,j,n_2} = z_{n_2}^{-1} J^* \left[\prod_{h=2}^{j-2} U_h\right] U_{j-1}(\alpha) U_j(\alpha\beta) U_{j+1}(\alpha\beta\gamma) \left[\prod_{h=j+2}^{n-1} U_h\right] J$$

where z_{n_2} is the partition function of the n_2th chain, the U matrices are arranged according to the configurational sequence as determined by the Monte Carlo method, $J^* = [1\ 0\ 0]$, J is the 9×1 matrix whose elements are unity, and n is the number of skeletal bonds in the chain. In $U_{j-1}(\alpha)$, the columns of the α state are equal to those of U_{j-1}, and the other elements are filled with zero. In $U_j(\alpha\beta)$, the elements corresponding to the $\alpha\beta$ conformation are filled with those of U_j, and the others are null. Similarly, the $U_{j+1}(\alpha\beta\gamma)$ matrix is defined. The bond lengths, bond angels, and dihedral angles are averaged according to

$$\bar{l}_A = \sum_{n_2}^{n_c} \sum_{j\in A} \sum_{\alpha} \sum_{\beta} \sum_{\gamma} l_{\alpha\beta\gamma,j,n_2} p_{\alpha\beta\gamma,j,n_2} \left(\sum_{n_2}^{n_c} \sum_{j\in A} \sum_{\alpha} \sum_{\beta} \sum_{\gamma} p_{\alpha\beta\gamma,j,n_2} \right)^{-1}$$

$$\bar{\theta}_B = \sum_{n_2}^{n_c} \sum_{j\in B} \sum_{\alpha} \sum_{\beta} \sum_{\gamma} \theta_{\alpha\beta\gamma,j,n_2} p_{\alpha\beta\gamma,j,n_2} \left(\sum_{n_2}^{n_c} \sum_{j\in B} \sum_{\alpha} \sum_{\beta} \sum_{\gamma} p_{\alpha\beta\gamma,j,n_2} \right)^{-1}$$

and

$$\bar{\phi}^D_{\beta,C} = \sum_{n_2}^{n_c} \sum_{j\in C} \sum_{j\in D} \sum_{\alpha} \sum_{\gamma} \phi_{\alpha\beta\gamma,j,n_2} p_{\alpha\beta\gamma,j,n_2} \left(\sum_{n_2}^{n_c} \sum_{j\in C} \sum_{j\in D} \sum_{\alpha} \sum_{\gamma} p_{\alpha\beta\gamma,j,n_2} \right)^{-1}$$

where A = CN, CC, or CX (X = O or S), B = CNC, NCC, CCX, or CXC, C = a, b, c, d, e, or f for PEIES, PEIEO, and PMEIEO, or a, b, or c for PEI, and D = *ll*, *dd*, *ld*, or *dl*. For example, the symbol, $j \in$ A, indicates that the summation is performed only when bond j corresponds to A. If low-energy chains with large z_{n_2}'s are accidentally generated, the $\langle r^2 \rangle$ value would be fluctuated. To avoid such errors, the characteristic ratio was calculated as the number average of the mean-square end-to-end distance $\langle M^2 \rangle_{n_2}$ (eq 1 of ref 5):

$$\langle r^2 \rangle_0 / nl^2 = \frac{\sum_{n_2=1}^{n_c} \langle M^2 \rangle_{n_2}}{n_c(l_1^2 + x\sum_C \bar{l}_C^2 + l_n^2)}$$

instead of as the weight average using the generation probability, $z_{n_2}/\sum_{n_2=1}^{n_c} z_{n_2}$, of the n_2th chain, where x is the degree of polymerization, l_C is the average length of bond C (defined as above). When n_c is fully large, the difference between the number- and weight-averages is negligible.

(23) On the ground described in section 4.4 of ref 5, the attractive interactions should be designated as attractions or attractive forces rather than hydrogen bonds. For consistency with our previous papers, however, the term "hydrogen bond strength" is used here.

(24) Strictly, the geometrical parameters are slightly changed with HBS. However, this effect has not been considered here. The molecular geometry at HBS = 100% was used in all the computations.

(25) Mattice, W. L.; Helfer, C. A.; Sokolov, A. P. *Macromolecules* **2004**, *37*, 4711.

MA071077B